

# Ultracold quantum gases in optical lattices

Artificial crystals of light, consisting of hundreds of thousands of optical microtraps, are routinely created by interfering optical laser beams. These so-called optical lattices act as versatile potential landscapes to trap ultracold quantum gases of bosons and fermions. They form powerful model systems of quantum many-body systems in periodic potentials for probing nonlinear wave dynamics and strongly correlated quantum phases, building fundamental quantum gates or observing Fermi surfaces in periodic potentials. Optical lattices represent a fast-paced modern and interdisciplinary field of research.

## IMMANUEL BLOCH

Institut für Physik, Johannes Gutenberg-Universität, D-55099 Mainz, Germany.

e-mail: [bloch@uni-mainz.de](mailto:bloch@uni-mainz.de)

Ultracold bosonic and fermionic quantum gases are versatile and robust systems for probing fundamental condensed-matter physics problems<sup>1–12</sup>, as well as finding applications in quantum optics and quantum information processing<sup>13</sup> and understanding atomic and molecular physics<sup>14,15</sup>. Storing such ultracold quantum gases in artificial periodic potentials of light has opened innovative manipulation and control possibilities, in many cases creating structures far beyond those currently achievable in typical condensed-matter physics systems. Amazingly, strong correlation effects can be observed in dilute atomic gases despite the densities of the particles in the trapping potentials being more than five orders of magnitude less than that of the air surrounding us! Ultracold quantum gases in optical lattices can in fact be considered as quantum simulators, as Richard P. Feynman originally conceived for a quantum computer: a powerful simulator in which a highly controllable quantum system can be used to simulate the dynamical behaviour of another complex quantum system<sup>16,17</sup>. As a simulator, an optical lattice offers remarkably clean access to a particular hamiltonian and thereby serves as a model system for testing fundamental theoretical concepts, at times providing textbook examples of quantum many-body effects.

### STORING NEUTRAL ATOMS IN OPTICAL POTENTIALS

Typically, ultracold neutral atoms are stored in magnetic traps, in which only a small subset of the available atomic spin states — the so-called weak-field-seeking states — can be trapped. This limitation is generally overcome by using optical dipole traps that rely on the interaction between an induced dipole moment in an atom and an external electric

field. Such a field can, for example, be provided by the oscillating electric light field from a laser, which induces an oscillating dipole moment in the atom while at the same time interacts with this dipole moment in order to create a trapping potential<sup>18</sup>  $V_{\text{dip}}(\mathbf{r})$  for the atoms:

$$V_{\text{dip}}(\mathbf{r}) = -\mathbf{d} \cdot \mathbf{E}(\mathbf{r}) \propto \alpha(\omega_L) |\mathbf{E}(\mathbf{r})|^2.$$

Here  $\alpha(\omega_L)$  denotes the polarizability of an atom and  $I(\mathbf{r}) \propto |\mathbf{E}(\mathbf{r})|^2$  characterizes the intensity of the laser light field, with  $\mathbf{E}(\mathbf{r})$  its electric field amplitude at position  $\mathbf{r}$ . The laser light is usually tuned far away from an atomic resonance frequency, such that spontaneous emission effects from resonant excitations can be neglected and the resulting dipole potential is purely conservative in nature. It can be attractive for laser light with a frequency  $\omega_L$  smaller than the atomic resonance frequency  $\omega_0$ , or repulsive for a laser frequency larger than the atomic resonance frequency.

A periodic potential can then be formed simply by overlapping two counter-propagating laser beams. The interference between the two laser beams forms an optical standing wave with period  $\lambda_L/2$ , which can trap the atoms. By interfering more laser beams, one can obtain one-, two- and three-dimensional (1D, 2D and 3D) periodic potentials. The 1D lattice, formed by a pair of laser beams, creates a single standing-wave interference pattern — effectively an array of 2D disk-like trapping potentials. Two orthogonal optical standing waves create an array of 1D potential tubes (see Fig. 1a), in which the atoms can only move along the weakly confining axis of the potential tube, thus realizing 1D quantum behaviour, with the radial motion being completely frozen out for low-enough temperatures. Three orthogonal optical standing waves correspond to a 3D simple cubic crystal (see Fig. 1b), in which each trapping site acts as a tightly confining harmonic oscillator potential.

One important advantage of using optical fields to create a periodic trapping potential is that the geometry and depth of the potential are under the

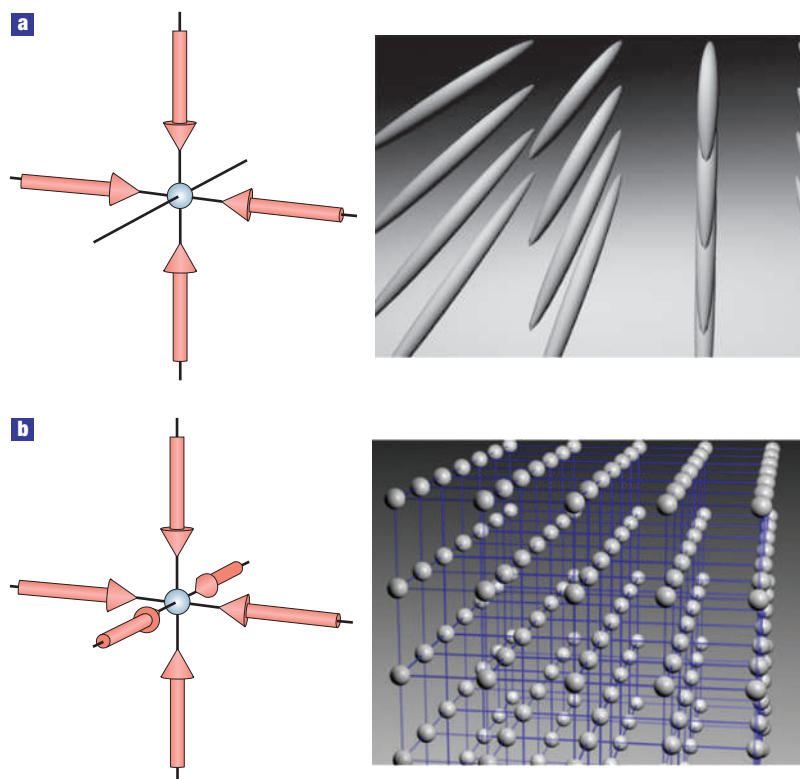


**Figure 1** Optical lattice potentials formed by superimposing two or three orthogonal standing waves. **a**, For a 2D optical lattice, the atoms are confined to an array of tightly confining 1D potential tubes. **b**, In the 3D case, the optical lattice can be approximated by a 3D simple cubic array of tightly confining harmonic oscillator potentials at each lattice site.

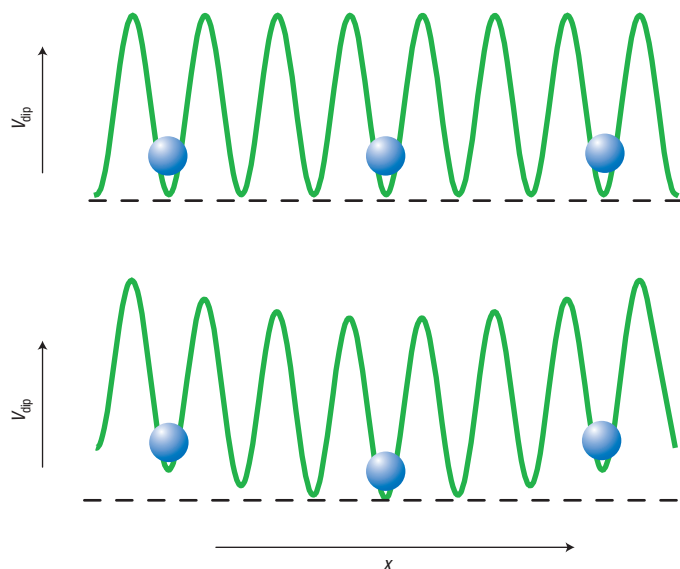


**Figure 2** Optical lattice potentials. **a**, The standing-wave interference pattern creates a periodic potential in which the atoms move by tunnel coupling between the individual wells. **b**, The gaussian beam profile of the lasers, a residual harmonic trapping potential, leads to a weak harmonic confinement superimposed over the periodic potential. Thus the overall trapping configuration is inhomogeneous.

complete control of the experimentalist. For example, the geometry of the trapping potentials can be changed by interfering laser beams under a different angle, thus making even more complex lattice configurations<sup>19</sup>, such as Kagomé lattices<sup>20</sup>. The depth of such optical potentials can even be varied dynamically during an experimental sequence by simply increasing or decreasing the intensity of the laser light, thus turning experimental investigations of the time dynamics of fundamental phase transitions into a reality.

Each periodic potential formed by a single standing wave has the form

$$V_{\text{lat}}(x) = V_0 \sin^2(k_L x),$$

where  $k_L = 2\pi/\lambda_L$  is the wave vector of the laser light used to form the optical standing wave and  $V_0$  represents the lattice potential depth, usually given in units of the recoil energy  $E_R = \hbar^2 k_L^2 / 2m$  ( $m$  being the mass of a single neutral atom), which is a natural energy scale for neutral atoms in periodic light fields. Note that by choosing to interfere two laser beams at an angle less than  $180^\circ$ , one can form periodic potentials with a larger period.

The motion of a single particle in such periodic potentials is described in terms of Bloch waves with crystal momentum  $q$ . However, an additional harmonic confinement arises due to the gaussian profile of the laser beams (see Fig. 2). Although this harmonic confinement is usually weak (typically around 10–200 Hz oscillation frequencies) compared with the confinement of the atoms on each lattice site (typically around 10–40 kHz), it generally leads to an inhomogeneous environment for the trapped atoms. One must be careful, therefore, when comparing experimental results derived for a homogeneous periodic potential case to the ones obtained under the inhomogeneous trapping conditions as described.

Owing to the large degree of control over the optical lattice parameters, a number of detection techniques have become available to directly measure the band populations present in the periodic potential. A good example of such a measurement technique is the mapping of a Bloch state in the  $n$ th energy band with crystal momentum  $q$  onto a free-particle momentum in the  $n$ th Brillouin zone (see Fig. 3). This can be achieved by adiabatically lowering the lattice potential depth, such that the crystal momentum of the excitation is preserved during ramp-down. Then, the crystal momentum is eventually mapped onto a free-particle momentum in the corresponding Brillouin zone<sup>21,22</sup> (see Fig. 3). For instance, for an equal statistical mixture of Bloch states in the lowest energy band, one expects a homogeneously filled momentum distribution of the atom cloud within the first Brillouin zone (a square in momentum space with width  $2\hbar k_L$ ). The atom cloud for such an input state should then expand like a square box after the adiabatic lowering of the optical lattice potential, which has indeed been observed experimentally<sup>22–24</sup>. Occupation of higher energy bands becomes visible as higher Brillouin zones are populated, and the atom cloud expands in a stair-case density distribution after adiabatic turn-off<sup>23</sup> (see Fig. 3e).

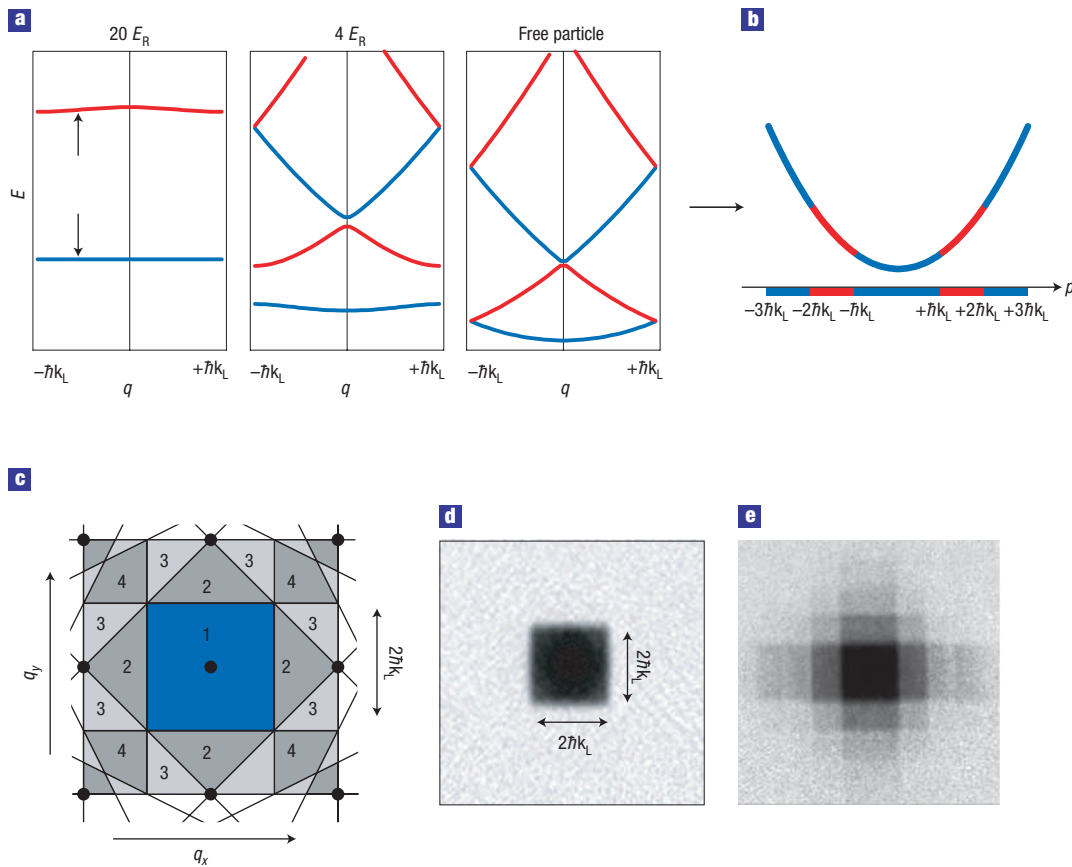


**Figure 3** Adiabatic mapping of crystal momentum onto free-space momentum of an atom. **a**, Bloch bands for different potential depths. During an adiabatic ramp-down the crystal momentum is conserved. **b**, A Bloch wave with crystal momentum  $q$  in the  $n$ th energy band is mapped onto a free particle with momentum  $p$  in the  $n$ th Brillouin zone of the lattice. **c**, 2D Brillouin zone scheme for a 2D simple cubic lattice configuration. **d**, Adiabatic mapping of a statistical mixture of Bloch states within the lowest energy band leads to the observation of a box-shaped expanding atom cloud, corresponding to a homogeneously filled central Brillouin zone. **e**, When the higher energy bands are occupied, populations of higher Brillouin zones become visible.

## NONLINEAR DYNAMICS IN PERIODIC POTENTIALS

For a weakly interacting Bose–Einstein condensate (BEC) in an optical lattice potential, the motion of the particles should at first sight resemble that of single particles moving in a periodic potential. However, the interactions between the particles, although weak, can lead to important nonlinear effects in the static and dynamic behaviour of the matter waves. For example, a BEC in a weak periodic potential can be described as an array of Josephson junctions<sup>25,26</sup>, with atom–atom interactions leading to nonlinear dynamics. Very recently, in a textbook experiment, researchers have been able to confine a BEC to just two wells of a periodic potential<sup>27</sup>, thus creating a double-well situation. The two condensates are coupled by a tunnelling potential through the barrier between the two sites. Such a double-well potential is effectively a single Josephson junction<sup>28–31</sup> for atomic quantum gases<sup>27</sup>. The small separation between the two lattice sites means a rather strong tunnel coupling between the two condensates, which brings the experimental timescale for the observation of the ensuing nonlinear dynamics into a measurable regime. The researchers measured the populations and phase difference of the two condensates in the double well (see Fig. 4) and observed two distinct regimes<sup>27</sup>. For a small initial population difference between the two lattice sites, the system showed clear Josephson oscillations in the population imbalance between the two sites, whereas for a large initial population

imbalance the system exhibited ‘self-trapping’, in which the initial population imbalance remained almost fixed over time ( $t$ ), and the phase difference ( $\varphi$ ) between the two condensates increased linearly over time due to the chemical potential ( $\mu$ ) difference between the condensates  $\varphi = (\mu_1 - \mu_2)t/\hbar$ .

The nonlinear interactions between particles in periodic potentials can also lead to pronounced instabilities that eventually destroy a BEC propagating through a periodic optical potential. This was recently demonstrated unambiguously<sup>32</sup>. A condensate in a weak optical potential was set into motion and propagated through an optical lattice. With increasing crystal momentum of the wavepacket, the researchers observed a sudden onset in the loss rate of condensed atom<sup>32</sup> (see Fig. 5). Amazingly, this happened close to the point at which the crystal momentum  $q$  is close to half of the reciprocal lattice vector  $q_B$ , that is,  $q/q_B \approx 0.5$ , providing strong evidence for the observation of the predicted dynamical instability behaviour<sup>33,34</sup>. Why does this instability occur close to these values of the crystal momentum? Intuitively this can be explained in the following way: for crystal momenta  $q > q_B/2$  the effective mass of the particles propagating through the lattice potential changes sign and becomes negative. A negative effective mass and repulsive interaction between the particles can be equally described by a system with positive effective mass but attractive interactions between the particles. However, the density distribution of a system with attractive interactions becomes unstable even for small population imbalances between



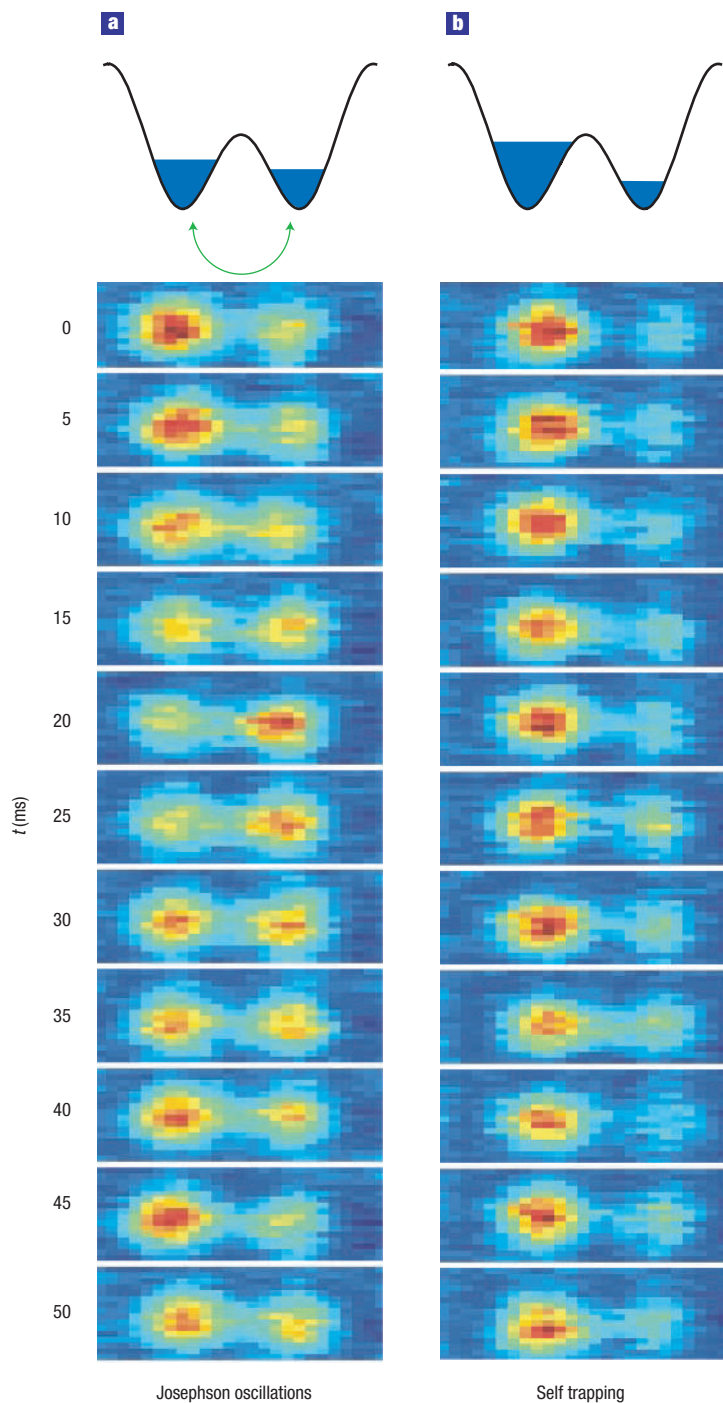


**Figure 4** Nonlinear dynamics for a BEC in a double-well system. **a**, For a small population imbalance between the two wells, Josephson oscillations between the two condensates in different wells are observed. **b**, For large population differences, the system enters a self-trapping mode, in which the population difference remains locked, but the phase difference between the two condensates increases linearly with time. With kind permission from M. Oberthaler, University of Heidelberg. Reprinted with permission from ref. 27. Copyright (2005) by the American Physical Society.

different wells, which leads to an enhancement of the density fluctuations. Consider the simpler case of a double-well system with attractive interactions; an equal population between particles in the left

and right potential well of the system will result in a metastable situation because the particles cannot decide which well to occupy in order to lower the total energy of the system. But for a small initial population imbalance between the wells, the particles will prefer to amplify this imbalance by moving into the well with more particles. The same effect acts on particles in the periodic potential. A small density fluctuation, which is always present in the system due to finite temperature effects, for example, will eventually be amplified and lead to the destruction of the condensate (see Fig. 5a).

## STRONGLY CORRELATED QUANTUM PHASES

Despite the presence of interactions between the particles trapped in an optical lattice, which lead to nonlinear terms in the Schrödinger-like equation known as the Gross–Pitaevskii equation<sup>35</sup>, a macroscopic wavefunction still very well describes the quantum many-body system in the weakly interacting regime. If the interactions become increasingly stronger relative to their kinetic energy, the system becomes strongly interacting and, in general, can no longer be described as a simple matter wave. The resulting strongly correlated quantum states are difficult to handle theoretically, and are extremely challenging for modern condensed-matter theory. A prominent example of such a transition from a weakly interacting quantum system to a strongly correlated quantum many-body system is the superfluid-to-Mott insulating state of matter for bosons<sup>1–4</sup>, originally predicted in a seminal work by Fisher *et al.*<sup>1</sup> and later introduced to ultracold atoms<sup>2</sup>. But how does this transition come about? If one considers only occupations of the lowest Bloch band, interacting bosons in optical potentials can be described by the Bose–Hubbard hamiltonian<sup>1</sup>

$$H = -J \sum_{\langle i,j \rangle} \hat{a}_i^\dagger \hat{a}_j + \frac{1}{2} U \sum_i \hat{n}_i (\hat{n}_i - 1).$$

The first term is the kinetic energy term, describing the tunnel coupling  $J$  between neighbouring lattice sites  $\langle i,j \rangle$  and  $\hat{a}_i^\dagger (\hat{a}_i)$  creates (destroys) a particle on lattice site  $i$ . The second term describes the onsite interactions  $U$  between the particles, with  $\hat{n}_i$  counting the number of particles on site  $i$ . Only when two particles are placed on the same lattice site can they interact with each other, leading to an interaction energy  $U$ . Such an interaction term works well for ultracold neutral atoms in periodic potentials, as their interactions are very short-ranged and no long-range Coulomb forces exist between the particles. This system exhibits two prominent ground states. For weak interactions relative to the kinetic energy  $U/J \ll 1$ , the system forms a Bose–Einstein condensed state of matter, where each atom is delocalized over the entire lattice. Such a state is favoured as the kinetic energy term is minimized for single-particle wavefunctions spread out throughout the lattice. In this case, the total system can be described by a giant matter wave and the atom number per lattice site follows a poissonian

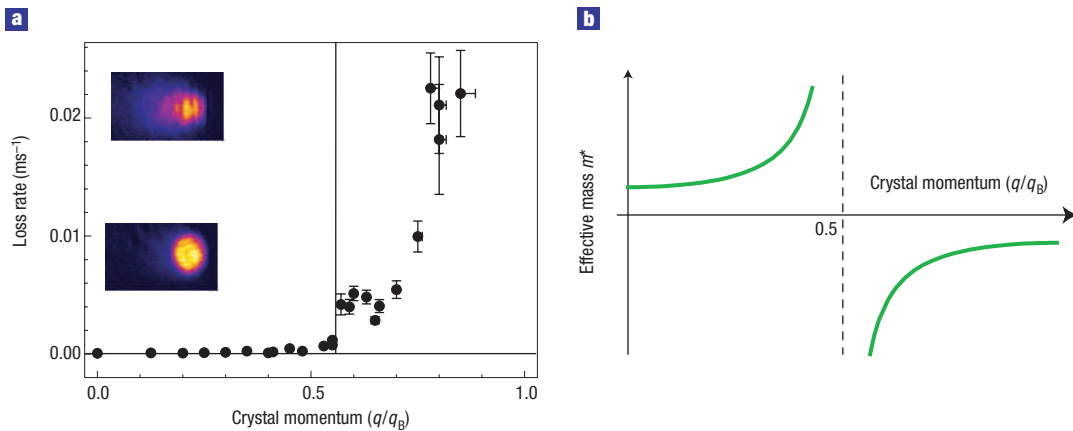


**Figure 5** Dynamical instability of a BEC in a periodic potential. **a**, For a movement of a BEC through a 1D optical lattice with a lattice depth of  $0.2E_R$  an instability is observed close to crystal momenta  $q/q_B > 0.5$ . With kind permission from M. Inguscio. Reprinted with permission from ref. 32. Copyright (2004) by the American Physical Society. **b**, This can be intuitively explained by a change of sign in the effective mass of the particles at  $q/q_B = 0.5$ , which is formally equivalent to a change of sign in the interaction strength between the atoms. Formerly repulsive interactions then become effectively attractive leading to an instability that destroys the condensate and leads to a large loss rate. Here  $q_B$  denotes the momentum at the band edge.

distribution. Upon sudden release of the matter wave from the optical lattice potential, one observes a multiple matter-wave interference pattern (see Fig. 6a). For the case of large interactions relative to the kinetic energy,  $U/J \gg 1$ , the system enters the strongly correlated state of a Mott insulator, in which the atoms are localized to single lattice sites, with a fixed particle number per site (see Fig. 6b). Therefore, the system cannot be described by a giant coherent matter wave, and for very strong interactions, no interference pattern can be observed upon releasing the particles from the lattice. Instead, perfect correlations in the particle number per site exist. Intriguingly, we found the timescale for the many-body system to switch from a Mott insulating state to a superfluid state to be of the order of a few tunnelling time constants<sup>3</sup>, which is remarkable considering the huge rearrangement of the system. Indeed, the dynamical evolution of the quantum many-body system across the transition remains an active and intriguing field of research, possibly even with analogues to cosmological phase transitions<sup>36,37</sup>.

Recently, Mott insulators in 1D have become attainable through the use of a deep 2D optical lattice loaded with a BEC<sup>6,38,39</sup>. The condensate then splits up into several thousand individual 1D BECs in each of the potential tubes. Subsequently, a third lattice potential applied along the direction of the tubes can drive the transition to the Mott insulating state, as explained above. For the one-dimensional case, a shift in the critical value for the transition in  $U/J$  was observed<sup>38</sup>, as predicted by theory. Surprisingly, the transport properties were already strongly affected well before the transition to a Mott insulator. One group<sup>40</sup> has recently investigated the oscillations of a 1D BEC along the weakly confining axes of the potential tubes in the presence of an additional lattice along the tubes, and found heavily damped oscillations for very shallow lattices, even before the system enters an insulating state, and such damping is expected. Although still somewhat puzzling, the effect has been attributed to zero-temperature quantum fluctuations, which are predicted to lead to significant damping in the 1D case<sup>41</sup>.

One-dimensional quantum systems are peculiar in many other respects. In 1960 Marvin Girardeau found<sup>5</sup> an exact mapping that relates the many-body

state of strongly interacting bosons with infinite repulsion between the particles (hardcore bosons) to the one of non-interacting fermions in an amazingly simple way:

$$\Psi_B(x_1, \dots, x_N) = |\Psi_F(x_1, \dots, x_N)|. \quad (1)$$

That is, the wavefunction of the strongly interacting hardcore bosons in 1D is nothing but the absolute value of the many-body wavefunction of the same number of non-interacting fermions! This remarkable mapping, known as fermionization, relies on the fact that the strongly interacting bosons in one dimension resemble non-interacting fermions. The strong repulsion between the particles effectively mimics Pauli's exclusion principle for fermions. Many properties of a fermionized Bose gas are identical to those of non-interacting fermions, such as their density distribution, though other properties, such as their momentum distribution, are distinctly different from both a non-interacting Fermi gas and a weakly interacting Bose gas. Initial evidence for such fermionic behaviour came from the observation of reduced three-body losses<sup>41</sup> for a 1D BEC approaching the strongly correlated regime of a Tonks–Girardeau gas. Furthermore, a shift of the collective excitation frequencies of the 1D gas was observed in this regime from the one expected for a 3D weakly interacting BEC, but still well described by 1D theories for weakly interacting condensates.

During the past year two groups were able to increase the interactions to a regime in which the measurements extend into the fermionized regime. This is again characterized by the ratio of interaction energy to kinetic energy, usually given by the parameter  $\gamma = E_{\text{int}}/E_{\text{kin}}$ . In a first experiment<sup>6</sup>,  $\gamma$  was increased by the addition of a weak lattice along the potential tubes, which amounts to an increase of the effective mass of the particles and, therefore, an increase in  $\gamma$  (up to 200). For low filling factors and  $\gamma \gg 1$ , the many-body quantum system enters the regime of a Tonks–Girardeau gas. Our group (see ref. 6) measured momentum distributions along the potential tubes, which are characteristic for a fermionized gas in 1D. We used a fermionization approach based on the mapping theorem of Girardeau (see equation 1) to explain the observed momentum distribution, obtaining good

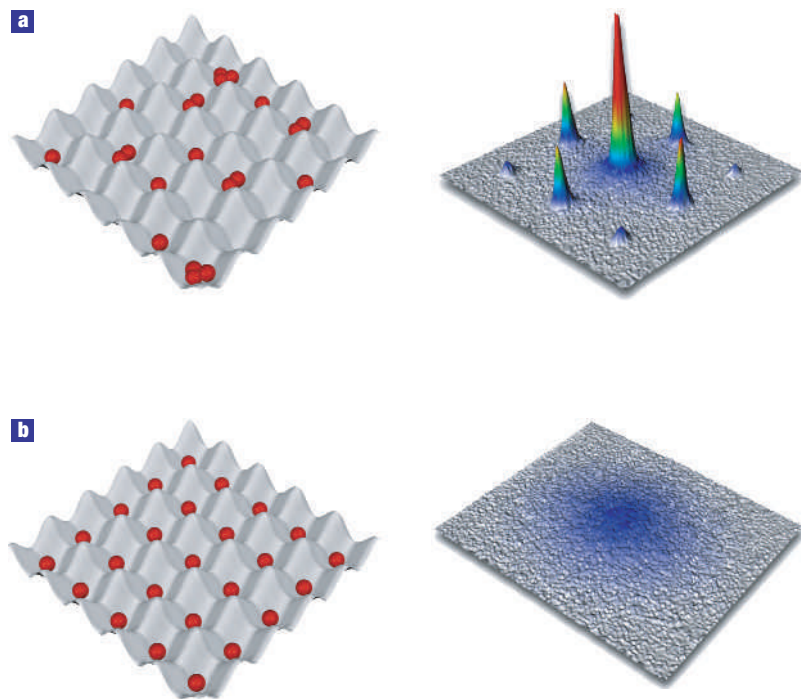


**Figure 6** Transition from a superfluid to a Mott insulator. **a**, In the superfluid state of a BEC, the underlying atoms can be described as a giant macroscopic matter wave. When such a condensate is released from the periodic potential, a multiple matter-wave interference pattern appears, owing to the phase coherence between the atomic wavefunctions on different lattice sites. In this case, the phase of the macroscopic matter wave is well defined. However, the atom number on each lattice site fluctuates. **b**, In the other limit of a Mott insulating state of matter, each lattice site is filled with a fixed number of atoms but the phase of the matter-wave field remains uncertain. No matter-wave interference can be seen in this case when the quantum gases are released from the lattice potential (see for example, ref. 3).

agreement between theory and experiment. In another experiment<sup>7</sup>, no further lattice was present along the direction of the tubes, but the confinement of the atoms in the radial direction was further increased, leading to values of  $\gamma$  of up to 5.5. They measured the 1D energy per particle and size of the atom clouds along the axial direction of the potential tubes and found good agreement with the exact results for the 1D case<sup>42</sup>, showing increasing deviations from the weakly interacting results upon increasing  $\gamma$ . In general, 1D quantum systems can be very well described by Luttinger-liquid theory<sup>43</sup>, applicable also in the intermediate regime for  $\gamma$ , which can be tested in future experiments. The realization of the quantum states of a Tonks–Girardeau gas emphasizes the versatility of ultracold quantum gases in the search for novel, or long-predicted quantum phases, which have so far eluded observation.

## FERMIONIC QUANTUM GASES IN OPTICAL LATTICES

Only recently have we begun to explore the potential of ultracold fermions in an optical lattice. In one of the pioneering experiments with fermions in 1D optical lattices, researchers studied the peculiar

transport properties of bosons and fermions in periodic potentials<sup>44</sup>. They found that applying steep potential gradients inhibited transport for fermions in optical lattices, but that collisions with added bosonic atoms can stimulate transport in the system again. In a different experiment<sup>45</sup> they also observed the onset of insulating behaviour in a trapped Fermi gas (a single-component Fermi gas) as the Fermi energy approaches the bandgap. For this, the researchers observed oscillations of their ultracold fermions in a 1D optical lattice, superimposed harmonic confinement and found that these oscillations were strongly suppressed for increased filling of the lowest energy band. In another very recent experiment<sup>24</sup>, ultracold fermionic <sup>40</sup>K atoms were loaded into a 3D optical lattice. Using the adiabatic mapping outlined above, they directly observed the Fermi surface of a Fermi gas (see Fig. 7). As the filling factor was increased, the fermionic system was driven into a band insulating state. The authors point out that such a band insulator, with one fermion per site, could also be used as a quantum register for quantum information purposes, as an alternative to a Mott insulator for bosonic atoms. The researchers also demonstrated that the usual restriction of atoms to the lowest Bloch band may break down if the interactions between two fermionic atoms in different spin states are increased such that the onsite interaction energy approaches the value of the vibrational splitting of the harmonic oscillator levels. Their impressive demonstration involved enhancing the interactions between two fermions in different spin states through a Feshbach resonance and observing the subsequent population of higher energy bands.

## OUTLOOK

What are the prospects for future investigations of ultracold atoms in optical lattices? I believe we have just cracked open the door to a wide interdisciplinary field of physics ranging from nonlinear dynamics to strongly correlated quantum phases and quantum information processing, which will provide us with many research highlights throughout the coming years. One natural step forward is to load spin-mixtures into the lattice potential. Theorists have predicted fascinating quantum phases, such as a counterflow superfluid<sup>46,47</sup>, for which the total density of a two-component spin-mixture in a lattice is fixed, but the individual spin components remain completely superfluid. Further predictions include Cooper-pair-like states<sup>48</sup>, possible ways to realize spin-Bose models<sup>49</sup> or even single-atom transistors<sup>50</sup> with neutral atoms. Moreover, by using spin-dependent lattice potentials one can map the hamiltonian of a two-component Bose mixture onto a controlled quantum-spin-system hamiltonian and investigate fundamental quantum magnetic systems<sup>46,51,52</sup> in a highly controllable environment.

Another research effort will be directed towards disordered systems<sup>53–56</sup>. Strongly interacting quantum systems in random potentials are among the most difficult systems to analyse theoretically. As one of the



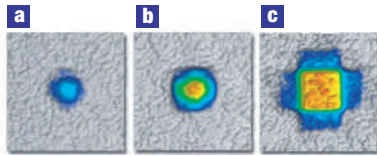


**Figure 7** Observing Fermi surfaces. **a–c**, Time-of-flight images of an ultracold Fermi gas of  $^{40}\text{K}$  atoms released from a 3D optical lattice potential for increasing filling factors corresponding to different Fermi energies. An adiabatic ramp-down of the lattice potential maps the crystal momentum of the particles onto free particle momentum, such that the band population can be directly observed in the time of flight absorption images (with kind permission from T. Esslinger, ETH Zurich, see also ref. 24).

highlights under discussion, theorists have predicted the existence of a Bose-glass phase<sup>1</sup>, an insulator without an energy gap, which should be observable experimentally. More recently, experimentalists have investigated random potentials in a 1D optical lattice, which were constructed by means of a laser speckle pattern, enabling them to measure the transport properties of a BEC in this random potential<sup>57</sup>. In addition to bosons, fermions in optical lattice potentials require further study in order for them to reveal their ‘hidden’ quantum phases. Fermions in a 3D optical lattice can be described by the famous Hubbard hamiltonian, which is believed to contain a possible explanation for high-temperature superconductivity<sup>58–60</sup>. Although this system has been investigated theoretically for decades, the exact form of the phase diagram remains unknown. Here, fermions in an optical lattice could be used to investigate this fundamental hamiltonian and find where antiferromagnetic and superfluid phases of fermions with repulsive interactions in periodic potentials are located<sup>60</sup>. Fermions in optical lattices are also suitable for precision interferometry measurements of the gravitational acceleration due to the absence of collisional shifts in single-species Fermi gases<sup>61</sup>.

In addition to single-species fermionic and bosonic gases, mixtures of bosonic and fermionic quantum gases in an optical lattice are predicted to contain exotic quantum phases<sup>20,53,56,62–65</sup>, which have never been observed in conventional condensed-matter physics. For example, several quantum phases consisting of composite fermions in superfluid or metallic phases have been found<sup>65</sup>. For many of the predicted strongly correlated quantum phases, it has not been clear how detectable they might be. The following clever idea could do the trick for many of those phases: quantum noise-correlations<sup>66</sup> in expanding atom clouds can reveal many ground states of the fermionic or bosonic atoms in optical lattices, for example, antiferromagnetic phases or charge-density waves. These noise correlations were recently observed simultaneously by two groups, using dissociating ultracold molecules<sup>67</sup> or Mott-insulator quantum gases in optical lattices<sup>68</sup> (see Fig. 8). We expect these quantum noise correlations to find many uses for the detection of other strongly correlated quantum phases. The discovery of such

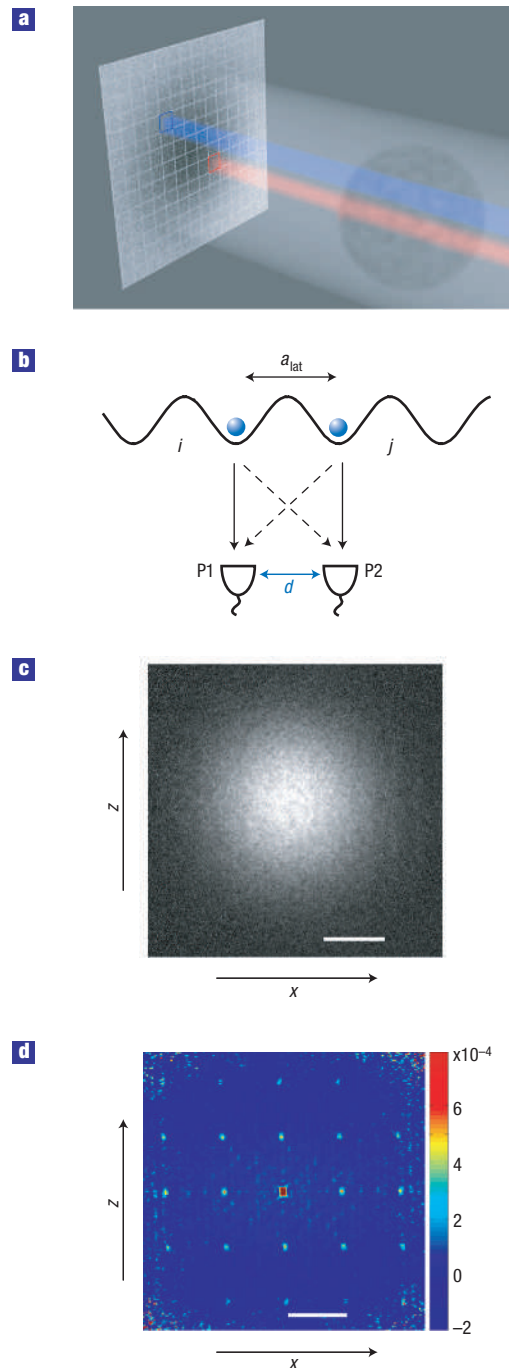


**Figure 8** Quantum noise correlations in atom clouds released from an optical lattice. **a**, Single absorption images of expanding atom clouds released from the lattice are recorded by absorption imaging. **b**, At two detectors (pixels) separated in space by a distance  $d$ , correlated detection events may occur at special separations, due to Hanbury Brown–Twiss type bunching of the atoms caused by the two paths along which two indistinguishable atoms can propagate to the detectors (dashed and solid lines).  $a_{\text{lat}}$  denotes the spacing of the atoms in the periodic potential. **c, d**, Whereas a single time-of-flight image of a released atom cloud from a Mott insulator, for example, does not show any structure (**c**), the second-order correlation function obtained from roughly a hundred of such single images (**d**), shows correlated detection events at special separations that reveal the ordering of the particles in the lattices (see also refs 66,68). The white scale bars in the image denote the length scale on which correlated detection events are predicted to occur.

quantum phases will advance our understanding of complex quantum matter under extreme conditions, undoubtedly bringing many exciting developments to our doorstep.

DOI:10.1038/NPHYS138

## REFERENCES

1. Fisher, M. P. A., Weichman, P. B., Grinstein, G. & Fisher, D. S. Boson localization and the superfluid-insulator transition. *Phys. Rev. B* **40**, 546–570 (1989).
2. Jaksch, D., Bruder, C., Cirac, J. I., Gardiner, C. W. & Zoller, P. Cold bosonic atoms in optical lattices. *Phys. Rev. Lett.* **81**, 3108–3111 (1998).
3. Greiner, M., Mandel, O., Esslinger, T., Hänsch, T. W. & Bloch, I. Quantum phase transition from a superfluid to a Mott insulator in a gas of ultracold atoms. *Nature* **415**, 39–44 (2002).

4. Orzel, C., Tuchman, A. K., Fenselau, M. L., Yasuda, M. & Kasevich, M. A. Squeezed states in a Bose-Einstein condensate. *Science* **291**, 2386–2389 (2001).
5. Girardeau, M. Relationship between systems of impenetrable bosons and fermions in one dimension. *J. Math. Phys.* **1**, 516–523 (1960).
6. Paredes, B. *et al.* Tonks–Girardeau gas of ultracold atoms in an optical lattice. *Nature* **429**, 277–281 (2004).
7. Kinoshita, T., Wenger, T. & Weiss, D. S. Observation of a one-dimensional Tonks–Girardeau gas. *Science* **305**, 1125–1128 (2004).
8. deMarco, B. & Jin, D. S. Onset of Fermi degeneracy in a trapped atomic gas. *Science* **285**, 1703–1706 (1999).
9. Truscott, A. G., Strecker, K. E., McAlexander, W. I., Partridge, G. B. & Hulet, R. G. Observation of Fermi pressure in a gas of trapped atoms. *Science* **291**, 2570–2572 (2001).
10. Regal, C., Greiner, M. & Jin, D. S. Observation of resonance condensation of fermionic atom pairs. *Phys. Rev. Lett.* **92**, 040403 (2004).
11. Chin, C. *et al.* Observation of the pairing gap in a strongly interacting Fermi gas. *Science* **305**, 1128–1130 (2004).
12. Zwierlein, M. W., Abo-Shaeer, J. R., Schirotzek, A., Schunck, C. H. & Ketterle, W. Vortices and superfluidity in a strongly interacting Fermi gas. *Nature* **435**, 1047–1051 (2005).
13. Bloch, I. Quantum gases in optical lattices. *Phys. World* **17**, 25–29 (2004).
14. Rom, T. *et al.* State selective production of molecules in optical lattices. *Phys. Rev. Lett.* **93**, 073002 (2004).
15. Ryu, C. *et al.* Raman-induced oscillation between an atomic and a molecular quantum gas. Preprint at <http://arxiv.org/abs/cond-mat/0508201> (2005).
16. Feynman, R. P. Quantum mechanical computers. *Opt. News* **11**, 11–20 (1985).
17. Feynman, R. P. Quantum mechanical computers. *Found. Phys.* **16**, 507–531 (1986).
18. Grimm, R., Weidemüller, M. & Ovchinnikov, Y. B. Optical dipole traps for neutral atoms. *Adv. At. Mol. Opt. Phys.* **42**, 95–170 (2000).
19. Petsas, K. I., Coates, A. B. & Grynberg, G. Crystallography of optical lattices. *Phys. Rev. A* **50**, 5173–5189 (1994).
20. Santos, L. *et al.* Atomic quantum gases in Kagomé lattices. *Phys. Rev. Lett.* **93**, 030601 (2004).
21. Kastberg, A., Phillips, W. D., Rolston, S. L. & Spreew, R. J. C. Adiabatic cooling of cesium to 700 nK in an optical lattice. *Phys. Rev. Lett.* **74**, 1542–1545 (1995).
22. Greiner, M., Bloch, I., Mandel, O., Hänsch, T. W. & Esslinger, T. Bose-Einstein condensates in 1D and 2D optical lattices. *Appl. Phys. B* **73**, 769–772 (2001).
23. Bloch, I. & Greiner, M. Exploring quantum matter with ultracold atoms in optical lattices. *Adv. At. Mol. Phys.* (in the press).
24. Köhl, M., Moritz, H., Stöferle, T., Günter, K. & Esslinger, T. Fermionic atoms in a 3D optical lattice: Observing Fermi-surfaces, dynamics and interactions. *Phys. Rev. Lett.* **94**, 080403 (2004).
25. Anderson, B. P. & Kasevich, M. A. Macroscopic quantum interference from atomic tunnel arrays. *Science* **282**, 1686–1689 (1998).
26. Cataliotti, E. S. *et al.* Josephson junction arrays with Bose-Einstein condensates. *Science* **293**, 843–846 (2001).
27. Albiez, M. *et al.* Direct observation of tunneling and nonlinear self-trapping in a single bosonic Josephson junction. *Phys. Rev. Lett.* **95**, 010402 (2005).
28. Josephson, B. D. Possible new effects in superconductive tunnelling. *Phys. Lett.* **1**, 251–253 (1962).
29. Likharev, K. K. Superconducting weak links. *Rev. Mod. Phys.* **51**, 101–159 (1979).
30. Pereverzev, S. V., Loshak, A., Backhaus, S., Davis, J. C. & Packard, R. E. Quantum oscillations between two weakly coupled reservoirs of superfluid  $^3\text{He}$ . *Nature* **388**, 449–451 (1997).
31. Sukhatme, K., Mukharsky, Y., Chui, T. & Pearson, D. Observation of the ideal Josephson effect in superfluid  $^4\text{He}$ . *Nature* **411**, 280–283 (2001).
32. Fallani, L. *et al.* Observation of dynamical instability for a Bose-Einstein condensate in a moving 1D optical lattice. *Phys. Rev. Lett.* **93**, 140406 (2004).
33. Wu, B. & Niu, Q. Landau and dynamical instabilities of the superflow of Bose-Einstein condensates in optical lattices. *Phys. Rev. A* **64**, 061603 (2001).
34. Smerzi, A., Trombettoni, A., Kevrekidis, P. G. & Bishop, A. R. Dynamical superfluid-insulator transition in a chain of weakly coupled Bose-Einstein condensates. *Phys. Rev. Lett.* **89**, 170402 (2002).
35. Pitaevskii, L. P. & Stringari, S. *Bose-Einstein Condensation* (Oxford Science, Oxford, 2003).
36. Zurek, W. H. Cosmological experiments in superfluid helium? *Nature* **317**, 505–508 (1985).
37. Zurek, W. H., Dorner, U. & Zoller, P. Dynamics of a quantum phase transition. *Phys. Rev. Lett.* **95**, 105701 (2005).
38. Stöferle, T., Moritz, H., Schori, C., Köhl, M. & Esslinger, T. Transition from a strongly interacting 1D superfluid to a Mott insulator. *Phys. Rev. Lett.* **92**, 130403 (2004).
39. Fertig, C. D. *et al.* Strongly inhibited transport of a degenerate 1D Bose gas in a lattice. *Phys. Rev. Lett.* **94**, 120403 (2005).
40. Polkovnikov, A. & Wang, D.-W. Effect of quantum fluctuations on the dipolar motion of Bose-Einstein condensates in optical lattices. *Phys. Rev. Lett.* **93**, 070401 (2004).
41. Laburthe-Tolra, B. *et al.* Observation of reduced three-body recombination in a correlated 1D degenerate Bose gas. *Phys. Rev. Lett.* **92**, 190401 (2004).
42. Lieb, E. H. & Liniger, W. Exact analysis of an interacting Bose gas. The general solution and the ground state. *Phys. Rev. B* **130**, 1605–1616 (1963).
43. Giamarchi, T. *Quantum Physics in One Dimension* (Oxford Science, Oxford, 2004).
44. Ott, H. *et al.* Collisionally induced transport in periodic potentials. *Phys. Rev. Lett.* **92**, 160601 (2004).
45. Pezzè, L. *et al.* Insulating behavior of a trapped Fermi gas. *Phys. Rev. Lett.* **93**, 120401 (2004).
46. Kuklov, A. & Svistunov, B. Counterflow superfluidity of two-species ultracold atoms in a commensurate optical lattice. *Phys. Rev. Lett.* **90**, 100401 (2003).
47. Kuklov, A., Prokof'ev, N. V. & Svistunov, B. Commensurate two-component bosons in an optical lattice: Ground state phase diagram. *Phys. Rev. Lett.* **92**, 050402 (2004).
48. Paredes, B. & Cirac, J. I. From Cooper pairs to Luttinger liquids with bosonic atoms in optical lattices. *Phys. Rev. Lett.* **90**, 150402 (2003).
49. Recati, A., Fedichev, P. O., Zwerger, W., von Delft, J. & Zoller, P. Atomic quantum dots coupled to a reservoir of a superfluid Bose-Einstein condensate. *Phys. Rev. Lett.* **94**, 040404 (2005).
50. Micheli, A., Daley, A. J., Jaksch, D. & Zoller, P. Single atom transistor in a 1D optical lattice. *Phys. Rev. Lett.* **93**, 140408 (2004).
51. Duan, L.-M., Demler, E. & Lukin, M. D. Controlling spin exchange interactions of ultracold atoms in an optical lattice. *Phys. Rev. Lett.* **91**, 090402 (2003).
52. Altman, E., Hofstetter, W., Demler, E. & Lukin, M. D. Phase diagram of two-component bosons on an optical lattice. *New J. Phys.* **5**, 113 (2003).
53. Roth, R. & Burnett, K. Ultracold bosonic atoms in two-color disordered optical superlattices. *J. Opt. B* **5**, S50–S54 (2003).
54. Roth, R. & Burnett, K. Phase diagram of bosonic atoms in two-color superlattices. *Phys. Rev. A* **68**, 023604 (2003).
55. Damski, B., Zakrzewski, J., Santos, L., Zoller, P. & Lewenstein, M. Atomic Bose and Anderson glasses in optical lattices. *Phys. Rev. Lett.* **91**, 080403 (2003).
56. Sanpera, A., Kantian, A., Sanchez-Palencia, L., Zakrzewski, J. & Lewenstein, M. Atomic Fermi-Bose mixtures in inhomogeneous and random lattices: From Fermi glass to quantum spin glass and quantum percolation. *Phys. Rev. Lett.* **93**, 040401 (2004).
57. Lye, J. E. *et al.* A Bose-Einstein condensate in a random potential. *Phys. Rev. Lett.* **95**, 070401 (2005).
58. Anderson, P. W. The resonating valence bond state in  $\text{La}_2\text{CuO}_4$  and superconductivity. *Science* **235**, 1196–1198 (1987).
59. Anderson, P. W. *et al.* The physics behind high-temperature superconducting cuprates: the 'plain vanilla' version of RVB. *J. Phys. Cond. Mat.* **16**, R755–R769 (2004).
60. Hofstetter, W., Cirac, J. I., Zoller, P., Demler, E. & Lukin, M. D. High-temperature superfluidity of fermionic atoms in optical lattices. *Phys. Rev. Lett.* **89**, 220407 (2002).
61. Roati, G. *et al.* Atom interferometry with trapped Fermi gases. *Phys. Rev. Lett.* **92**, 230402 (2004).
62. Büchler, H. P. & Blatter, G. Phase separation of atomic Bose-Fermi mixtures in an optical lattice. *Phys. Rev. A* **69**, 063603 (2004).
63. Albus, A., Illuminati, F. & Eisert, J. Mixtures of bosonic and fermionic atoms in optical lattices. *Phys. Rev. A* **68**, 023606 (2003).
64. Roth, R. & Burnett, K. Quantum phases of atomic boson-fermion mixtures in optical lattices. *Phys. Rev. A* **69**, 021601(R) (2004).
65. Lewenstein, M., Santos, L., Baranov, M. A. & Fehrmann, H. Atomic Bose-Fermi mixtures in an optical lattice. *Phys. Rev. Lett.* **92**, 050401 (2004).
66. Altman, E., Demler, E. & Lukin, M. D. Probing many-body states of ultracold atoms via noise correlations. *Phys. Rev. A* **70**, 013603 (2004).
67. Greiner, M., Regal, C. A., Stewart, J. T. & Jin, D. S. Probing pair-correlated fermionic atoms through correlations in atom shot noise. *Phys. Rev. Lett.* **110**, 110401 (2005).
68. Fölling, S. *et al.* Spatial quantum noise interferometry in expanding ultracold atomic gases. *Nature* **434**, 481–484 (2005).